

Optimization of a Solid Oxide Fuel Cell With A New Multi-fidelity Deep Stochastic Collocation for Spatial Outputs

²Wei Xing, ^{1*}Akeel A. Shah, ³Guohao Dai, ³Hong Qiu

¹ Key Laboratory of Low-grade Energy Utilization Technologies and Systems, Chongqing University, Chongqing 400030, China

² School of Microelectronics, Beijing University of Aeronautics and Astronautics, Xueyuan Road, Haidian 100191, China

³ College of Mechatronics and Control Engineering, Shenzhen University, 3688 Nanhai Avenue, Nanshan 518060, China

* E-mail: akeelshah@cqu.edu.cn

Abstract

Modelling and simulation play a major role in the design and optimization of solid oxide fuel cells (SOFC). We present a new flexible method for multi-fidelity optimization of SOFCs based on spatial-output stochastic collocation (SC) enhanced with deep learning to extract key features. In contrast to virtually all previous approaches to optimization of SOFC, we consider spatial outputs, which provide crucial detailed information and allow for the optimization of multiple objectives. Even though SC is highly accurate compared to other methods such as autoregression, this comes at the cost of requiring the exact low-fidelity results for making predictions. We therefore use a spatial-output Gaussian process model for the lowest fidelity. The method is validated on a complex 3-d SOFC model and used for optimization. It is shown to be more accurate than SC, even without the exact low-fidelity result for predictions, leading to massive reductions in computational cost and simultaneously very high accuracy.

Keywords: Solid oxide fuel cell; design optimization; spatial outputs; multi-fidelity model; stochastic collocation; deep learning.

I. Introduction

Fuel cells (FCs) are expected to play a major role in the future energy landscape, including as standalone power and for electric vehicle propulsion. FCs convert chemical energy into electricity [5] generating benign products such as water. Solid oxide fuel cells (SOFC) are highly attractive due to their fuel flexibility, high temperatures allowing for combined heat and power, low cost and range of different geometries. Modelling and simulation are important tools in the development of fuel cells, providing fundamental insights and lowering the costs associated with laboratory investigations, particularly for design and optimization. Detailed fuel cell models, however, involve a complex system of nonlinear differential equations, making them prohibitive for applications requiring results at many parameter values, e.g., optimization. Surrogate model approximations are often used instead, based on machine learning and/or multi-fidelity methods. Surrogate models for spatial outputs are particularly challenging due to dataset sizes, but are much more informative for design and optimization, e.g., for ensuring uniform flow/temperature, and the capability to optimise multiple quantities defined by the spatial outputs. Machine learning has been used extensively as surrogate models for electrochemical devices, for sensitivity analysis [1], optimization [2], health monitoring, and inverse parameter estimation, usually based on linear regression [3], artificial neural networks (ANN) [4] and, more recently, deep neural networks (DNN) [5] and Gaussian process (GP) models [6].

In multi-fidelity modelling (usually based on machine learning), models of different fidelity are combined in such a way that predictions at high fidelity are possible with few high-fidelity examples. The autoregressive (AR) multi-fidelity model assumes a parametric mapping between different fidelity levels. Nonlinear AR [7] places GP priors over the cross-fidelity mappings, increasing model complexity. An obvious drawback, however, is that the lower fidelity solution is an input to the higher fidelity GP model, making it unfeasible for high-dimensional output spaces. Furthermore, expensive sampling or variational methods are required for training and inference. In the highly-accurate multi-fidelity stochastic collocation (SC) method of [8], a small number of high-fidelity simulations are conducted based on a greedy criterion and the low-fidelity results are used to approximate the coefficients in a high-fidelity interpolation. This approach, on the other hand, requires out-of-sample low-fidelity model results in order to make predictions. The main drawback of SC is that it is essentially equivalent to applying Bayesian linear regression to approximate the mapping between low- and high-fidelity simulations, which limits its model capacity.

In this paper we develop a surrogate model for an SOFC that can be used for optimization purposes and is capable of approximating detailed spatial information. The great advantage of approximating spatial information is that: (a) it can be used for a detailed general analysis; and (b) optimization with respect to multiple objectives. A detailed 3-d SOFC model that includes mass, momentum and charge balances is simulated. The SC approach is extended by introducing a novel feature engineering step that leverages the latest advances in DNNs to efficiently extract features that enhance the predictions. In order to avoid low-fidelity simulations for making predictions, a GP model is used to learn the low fidelity map. We show that this method is superior to the original SC and to AR approaches when applied to the SOFC model. We then apply the new deep SC method to engineering design optimization of the SOFC to validate the results based on the original physics-based model.

II. Solid oxide fuel cell physics-based model

We consider a realistic, detailed steady-state 3-d solid oxide fuel cell model with different fidelity settings. The domain is single anode and cathode channels, the electrodes and a ceramic separator. The model includes charge balances in the electrolyte and electrodes, Navier Stokes equations for the gas channel flow, Brinkman's equation

for porous electrode flow, and mass balances in the channels and electrodes (Maxwell-Stefan diffusion). Butler-Volmer kinetics are used for the electrochemical reactions, with potentiostatic operation. A two-fidelity setting was considered. The model was implemented in COMSOL Multiphysics based on the finite element method. The low-fidelity (high-fidelity) model used 3164 (37064) mapped elements with a relative tolerance of 0.1 (0.001).

$N = 60$ simulations were performed at each fidelity with 4 inputs chosen using a Sobol sequence. The inputs were the electrode porosities $0.4 \leq \varepsilon \leq 0.85$, the cell voltage $0.055 \leq E \leq 0.7$ V, the temperature $973 \leq T \leq 1273$ K, and the channel pressures $0.5 \leq P \leq 2.5$ atm. The inputs are collected in a vector $\xi_n = (\varepsilon_n, E_n, T_n, P_n)$, $n = 1, \dots, N$. 40 further simulations at high-fidelity were conducted in order to test the accuracy of the method. The outputs were vectorised values of the electrolyte current density $i_e(\mathbf{x}; \xi)$ (A m⁻²) and the ionic potential $\phi_e(\mathbf{x}; \xi)$ (V) in a 2-d plane midway along the channel, at $j = 1, \dots, d = 5000$ locations \mathbf{x}_j . The outputs are denoted $\mathbf{y}_{f,n} \in \mathbb{R}^d$, where $f = 1, 2$ denotes the fidelity level (1 for low, 2 for high) and $n = 1, \dots, N$ indicates the input ξ_n .

III. Deep stochastic collocation multi-fidelity model for SOFC spatial outputs

The stochastic collocation approach [18] finds an estimator $\mathbf{y}_2 = f_2(\xi)$ of the high-fidelity model of the form

$$\mathbf{y}_2 = \sum_{k=1}^m c_k(\xi) \mathbf{y}_{2,k} \quad (1)$$

in which $m \leq N$ is the number of training points, \mathbf{y}_2 is the prediction for a general ξ and $c_k(\xi)$ are coefficients that depend on ξ . First, $\xi_n, n = 1, \dots, M \leq N$ points are selected to generate a candidate set Ω of inputs. Using a greedy procedure, a subset $Y \subset \Omega$ of $m < M$ points are selected amongst this candidate set to form the set of high-fidelity simulations to use. This is achieved by selecting a first point $\xi_j \in \Omega$ and setting $Y_1 = \{\xi_j\}$, finding $\xi_* = \operatorname{argmax}_{\xi_n \in \Omega} d_1$ and setting $Y_2 = Y_1 \cup \{\xi_*\}$, in which $d_1 = \min_{\xi_i \in Y_1} \|\xi_n - \xi_i\|$ minimizes the distance between ξ_n and Y_1 . We then find $\xi_* = \operatorname{argmax}_{\xi_n \in \Omega} d_2$ with $d_2 = \min_{\xi_i \in Y_2} \|\xi_n - \xi_i\|$ and set $Y_3 = Y_1 \cup \{\xi_*\}$. This process is repeated until the set $Y_3 = Y$ is generated with m samples.

Given a new \mathbf{y}_1 corresponding to a general ξ , the coefficients $c_k(\xi)$ are determined by the conditions $\sum_{k=1}^m c_k(\xi) \mathbf{y}_{1,k}^T \mathbf{y}_{1,n} = \mathbf{y}_1^T \mathbf{y}_{1,n}$ for all $\mathbf{y}_{1,n} \in Y$. This is an interpolation or projection of \mathbf{y}_1 onto the span of the low fidelity solutions $\mathbf{y}_{1,n} \in Y$. In practice, the stochastic collocation approach is equivalent to a Gaussian process model with linear kernel and the high-fidelity prediction can be expressed as

$$\mathbf{y}_2 = f_2(\mathbf{y}_1) = \mathbf{Y}_2 (\mathbf{Y}_1^T \mathbf{Y}_1)^{-1} \mathbf{Y}_1^T \mathbf{y}_1; \quad \mathbf{Y}_f = [\mathbf{y}_{f,1} \dots \mathbf{y}_{f,N}] \in \mathbb{R}^{d \times N} \quad (2)$$

Rather than solely relying on \mathbf{y}_1 as the input, we proposed a feature engineering approach such that

$$\mathbf{y}_2 = f_2(\mathbf{y}_1) = \mathbf{Y}_2 (\hat{\mathbf{Y}}_1^T \hat{\mathbf{Y}}_1)^{-1} \hat{\mathbf{Y}}_1^T \hat{\mathbf{y}}_1 \quad (3)$$

where $\hat{\mathbf{y}}_1 = [\mathbf{y}_1 \mathbf{z}]$ augments (enhances) \mathbf{y}_1 by concatenating it with a feature vector \mathbf{z} . $\hat{\mathbf{Y}}_1 = [\hat{\mathbf{y}}_{1,1} \dots \hat{\mathbf{y}}_{1,N}]$ is formed from the concatenated vectors $\hat{\mathbf{y}}_{1,1} = [\mathbf{y}_{1,1} \mathbf{z}_1]$ corresponding to the data points. The features \mathbf{z}_n and \mathbf{z} are learned using a DNN that has inputs $\mathbf{y}_{1,n}$ and targets $\mathbf{y}_{2,n}, n = 1, \dots, m$. They are taken as the outputs of the final hidden layer. We write the result compactly as $\mathbf{z}_n = \text{DNN}(\mathbf{y}_{1,n})$ and $\mathbf{z} = \text{DNN}(\mathbf{y}_1)$. This procedure reveals important latent features that can be used as inputs to enhance the predictive power of SC. The DNN can be a convolutional, recurrent or multi-layer perceptron network (CNN, RNN, MLP). We note that the computational complexity of SC is $O(m^3)$. Thus, our feature engineering approach does not significantly increase complexity.

The major drawback of the SC approach is the requirement for a full model evaluation of an out of sample \mathbf{y}_1 corresponding to ξ . In order to circumvent this problem, we learn a mapping $\mathbf{y}_1 = f_1(\xi)$ using a GP model. Specifically, we place a GP prior over $f_1(\xi)$ with a separable covariance structure

$$f_1(\xi) \sim \mathcal{GP}(f_2(\xi) | \mathbf{0}, k(\xi, \xi' | \boldsymbol{\theta}) \otimes \mathbf{B} + \sigma^2 \delta(\xi, \xi') \otimes \mathbf{I}) \quad (4)$$

in which the first and second arguments are the mean and covariance functions. $k(\xi, \xi' | \boldsymbol{\theta})$ captures the covariance across ξ , dependent on hyperparameters $\boldsymbol{\theta}$, $\mathbf{B} \in \mathbb{R}^{d \times d}$ is the covariance matrix across components of $f_1(\xi)$, and \otimes is a tensor product. The term $\sigma^2 \delta(\xi, \xi') \otimes \mathbf{I}$, in which $\delta(\xi, \xi')$ is a delta function, is included for numerical stability. The hyperparameters $\{\boldsymbol{\theta}, \mathbf{B}, \sigma^2\}$ are learned by a maximum log likelihood of the data $\mathbf{y}_{1,n}, \xi_n, n = 1, \dots, M$.

The method can be extended by a recursive application from fidelity $f = 1$ to $f = F > 2$. The DNN training requires a large data set to prevent overfitting, which presents a problem at high values of f . Therefore, we introduce a long-short-term-memory (LSTM) network that modifies the features at f to learn the features at $f + 1$, retaining information at all f values. Specifically, $\mathbf{z}_1 = \text{DNN}_1(\mathbf{y}_1)$, which learns the key features from the lowest-fidelity simulation. We then learn the features $\mathbf{z}_{f+1}, f = 1, \dots, F - 1$ from $\mathbf{z}_{f+1} = \text{LSTM}(\mathbf{z}_f)$, in which $\text{LSTM}(\mathbf{z}_f)$ denotes the final hidden layer output from an LSTM network with inputs \mathbf{z}_f and outputs $\mathbf{y}_{f+1,n}$.

Optimization of SOFC design. Optimization of the SOFC, namely any functional $g(\mathbf{y}_F)$ of the output \mathbf{y}_F was performed with gradient decent. The Jacobian of \mathbf{y}_F was computed though the chain rule $J_{\mathbf{y}_F}(\xi) = J_{f_F}(\mathbf{y}_{F-1}) \dots J_{f_2}(\mathbf{y}_1) J_{f_1}(\xi)$, with $f_1(\xi)$ obtained from Eq. (4) and the $f_f(\mathbf{y}_{f-1})$ from Eq. (3).

IV. Results and Discussion

The multi-fidelity model was implemented on the bi-fidelity SOFC data described earlier with a CNN for the feature learning, with one hidden layer and 256 filters of size 100. The root mean square errors (RMSE) for different high-

and low-fidelity training point numbers are shown in Fig. 1. As can be see, the deep SC approach is more accurate at all training point numbers than SC. The improvement may not appear significant, but it is important to realise that the original SC uses the original low-fidelity model to make a prediction. In our method we replace this highly expensive step by a fast GP approximation ($<0.1s$), while still exceeding the accuracy.

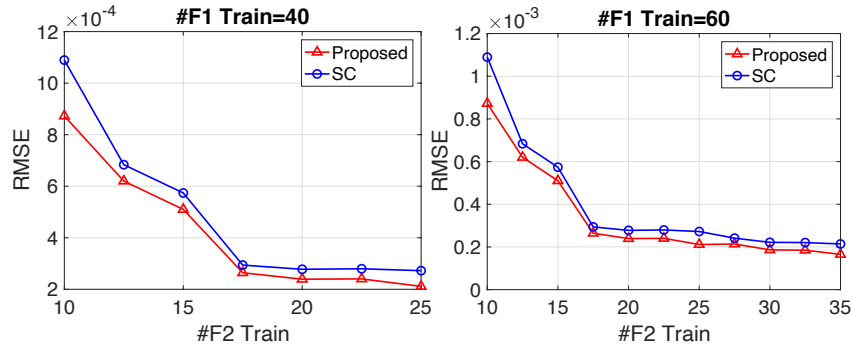


Fig. 1: RMSE for the proposed method and the classic SC trained using different number of training samples for the two-fidelity SOFC ionic potential output. #F1 Train and #F2 Train indicate the number of training samples for low- and high-fidelity.

Optimization was performed using gradient descent with constraints $0.4 \leq \varepsilon \leq 0.85$, $973 \leq T \leq 1273$, K , $0.055 \leq E \leq 0.7$ V, $0.5 \leq P \leq 2.5$ atm. To illustrate we used the average value of $\phi_e(\mathbf{x}; \xi)$ as the objective function and sought $\xi_* = \operatorname{argmax}_{\xi} \int \phi_e(\mathbf{x}; \xi) d\mathbf{x}$, approximated with a trapezoidal rule. The original SC is compared with the deep SC and the exact result (using the original high-fidelity model) in Tab. 1. As can be seen deep SC achieves high accuracy, whereas SC provides poor approximations of the true porosity and pressures.

Tab.1: Values of $\xi_* = \operatorname{argmax}_{\xi} \phi_e(\mathbf{x}; \xi)$ for deep SC and SC, together with the exact value.

	ε	T	E	P
Exact ξ_*	0.84998	1272.98	0.05501	1.27483
Deep SC ξ_*	0.84648	1270.66	0.05508	1.26263
SC ξ_*	0.40432	1261.19	0.05508	1.48584

V. Conclusions

Multi-fidelity modelling is a promising route to optimization, sensitivity analysis and uncertainty quantification of SOFC systems, as well as other fuel cells and batteries. It dramatically cuts the requirement for high fidelity examples compared to pure machine learning approaches. SC is known to be highly accurate, but at the cost of full model simulations at low fidelity for each prediction. This is usually unfeasible for the aforementioned applications, in which 100's to 10,000's of simulations are required. By using a feature engineering approach based on deep learning and a GP model at low-fidelity we are able to exceed the accuracy of SC. In a full paper we present the results on larger data sets and more quantities, a three-fidelity example, and comparisons to autoregression.

References

- [1] A. Kriston, A. Podias, I. Adanouj, and A. Pfrang. Analysis of the effect of thermal runaway initiation conditions on the severity of thermal runaway-numerical simulation and machine learning study. *J. Electrochem. Soc.*, 167(9):090555, 2020.
- [2] Majdi I. Radaideh, Mohammed I. Radaideh, and Tomasz Kozlowski. Design optimization under uncertainty of hybrid fuel cell energy systems for power generation and cooling purposes. *Int. J. Hydrogen Energy*, 45(3):2224 – 2243, 2020.
- [3] A. Maheshwari, M. A. Dumitrescu, M. Destro, and M. Santarelli. Inverse parameter determination in the development of an optimized lithium iron phosphate-graphite battery discharge model. *J. Power Sources*, 307:160 – 172, 2016.
- [4] M. Peksen, L. Blum, and D. Stolten. Optimisation of a solid oxide fuel cell reformer using surrogate modelling, design of experiments and computational fluid dynamics. *Int. J. Hydrogen Energy*, 37:12540 – 12547, 2012.
- [5] X. Zhang, J. Zhou, and W. Chen. Data-driven fault diagnosis for pemfc systems of hybrid tram based on deep learning. *Int. J. Hydrogen Energy*, 45(24):13483–13495, 2020.
- [6] P. Tagade, K.S. Hariharan, S. Ramachandran, A. Khandelwal, A. Naha, S.M. Kolake, and S.H. Han. Deep gaussian process regression for lithium-ion battery health prognosis and degradation mode diagnosis. *J. Power Sources*, 445:227281, 2020.
- [7] P. Perdikaris, M. Raissi, A. Damianou, N. Lawrence, G. E. Karniadakis, Nonlinear information fusion algorithms for data-efficient multi-fidelity modelling, *Proc. Roy. Soc. A*, 473 (2017) 20160751.
- [8] A. Narayan, C. Gittelsohn, D. Xiu, A stochastic collocation algorithm with multifidelity models, *SIAM J. Sci. Comp.* 36 (2014) A495–A521.